25p I 5
(招待講演)

RECENT ADVANCES IN TUNABLE MID-INFRARED LASER SOURCES FOR ENVIRONMENTAL GAS MONITORING

F. K. TITTEL, K. P. PETROV, R. F. CURL
Departments of Electrical and Computer Engineering and Chemistry
Rice University, Houston, TX 77251-1892 U.S.A.

L. GOLDBERG, W. K. BURNS
Naval Research Laboratory, Washington, D.C. 20375-5670 U.S.A.

S. WALTMAN, E. J. DLUGOKENCKY, L. W. HOLLBERG
National Institute of Standards and Technology, 325 Broadway, Boulder, CO 80303 U.S.A.

In this paper, a summary of recent advances in room-temperature tunable mid-infrared laser technology is presented. The two experiments discussed herein have been motivated by the growing need of compact all-solid-state CW sources in the 3 to 18 μm wavelength range. This range contains strong fundamental molecular absorption bands of many organic and inorganic air pollutants, and can be used for real-time sensitive measurement of these pollutants *in situ* and over long path. Lead-salt diode based trace gas detection in the mid-infrared have been recently demonstrated by Webster *et al* [1], and can be used as an alternative to near-infrared overtone detection [2]. Lead-salt diode lasers, however, require cooling with liquid nitrogen for normal operation which may be a practical drawback. An alternative to lead-salt diodes are multiple-quantum-well antimonide diode lasers [3]. Their performance characteristics such as operating temperature, spectral purity, and output power, have dramatically improved in recent years. Further research and development in this area can potentially result in simple and reliable single-frequency CW sources in the 3 to 5 μm region with tens of milliwatts of output power, operated at room or thermoelectric temperatures. Another important technique for generation of tunable infrared light are continuous-wave OPO [4] and DFG [5]. The DFG pumped by near-infrared semiconductor lasers [6-8], in our opinion, offers a clear advantage of stable single longitudinal mode operation, good amplitude and frequency stability, and wide continuous tuning range. To investigate the applicability of DFG to trace gas detection, we have built and tested two tunable infrared sources: one near 3.2 for the detection of methane, the other near 4.6 μm for the detection of carbon monoxide and nitrous oxide. Schematic diagrams of these sources are shown in Figure 1.

The 3.2 μm source was pumped by two different compact lasers: a 500 mW diode-pumped monolithic Nd:YAG ring laser at 1064 nm (signal), and a 20 mW extended-cavity diode laser (ECDL) at 800 nm (pump). In later experiments, the ECDL was replaced with a 100 mW solitary Fabry-Perot diode laser in order to increase the IR output power and allow fast wavelength modulation. The lasers were mixed in a 5.5 mm antireflection-coated $AgGaS_2$ placed inside a bow-tie enhancement cavity. The cavity was locked to resonance at 1064 nm to increase effective signal power available for mixing. The long arm of the cavity was not a conventional bow-tie in that a Littrow prism reflector was used instead of a flat mirror. The function of this element was to eliminate multiple passes of the 800 nm light in the cavity. Use of a flat mirror resulted in a small portion of the diode laser light circulating in the cavity which produced a systematic ripple in the IR power when the diode was tuned. The bow-tie cavity design with the addition of a Littrow prism reflector provides several advantages: it employs a minimum number of intracavity elements, is easy to align, has flexible mode diameter control, which is important for reaching optimum DFG conversion efficiency, and eliminates cavity resonance at the pump wavelength. The source was scanned by sweeping the frequency of the ECDL or solitary laser diode.

The 3.2 μm output beam (idler) was monitored using two room-temperature InAs detectors. A maximum of 6 μW IR power was measured with 40 mW pump power incident on the crystal, and 230 mW signal power in front of the cavity, which corresponds to 3.75 W intracavity signal power. Operation with more than 4.2 W intracavity Nd:YAG power was achieved, accompanied by noticeable thermal lensing in the mixing crystal. Frequency tuning of the idler wave was performed by tuning of the pump laser and crystal angle. At a fixed phase matching angle, frequency tuning over a range of approximately 10 cm^{-1} was possible, due to small crystal length. Therefore, short frequency scans of 10 GHz for spectroscopic measurements did not require crystal rotation. Tuning of the pump laser

from 801.3 nm to 795.2 nm and changing the internal phase matching angle of the crystal from 80° to 90° shifted the peak output IR power from 3076 cm^{-1} to 3183 cm^{-1}. Operation at infrared frequencies below 3076 cm^{-1} was possible with phase matching angles below 80° but at the cost of more than 25% reduction in the output power due to larger beam walk-off, decreasing effective nonlinear coefficient, and increasing Fresnel reflection losses at the AR-coated crystal surfaces which decreased the cavity buildup.

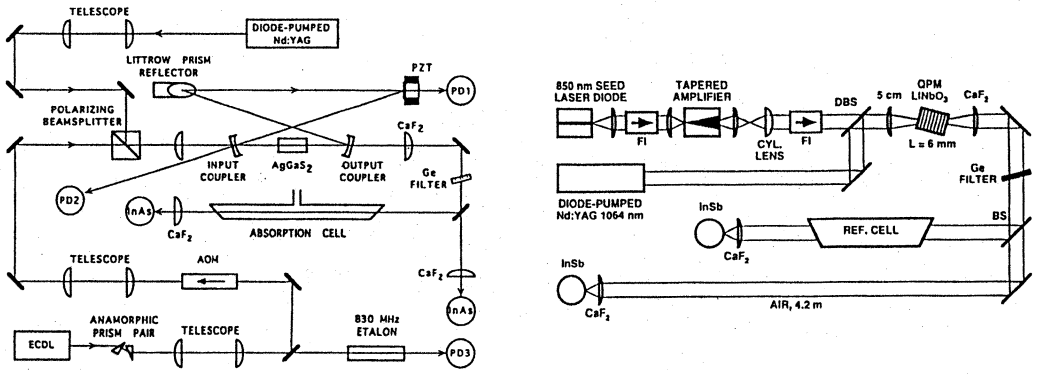

Figure 1. Diode-pumped cavity-enhanced 3.2 μm DFG source based on $AgGaS_2$ (**left**) and single-pass 4.6 μm DFG source using periodically poled $LiNbO_3$ (**right**). Both generated more than 6 μW infrared light tunable over 200 cm^{-1} with less than 50 MHz linewidth and were used for detection of methane and carbon monoxide in natural air.

The 4.6 μm source used a lower power version of the diode-pumped Nd:YAG ring laser mentioned above. It was mixed with an optically seeded high-power tapered GaAlAs semiconductor amplifier. The Fabry-Perot seed laser was isolated from the tapered amplifier by a 40 dB Faraday isolator and temperature-stabilized to ±0.02 °C, yielding frequency stability of ±0.6 GHz. To eliminate feedback-induced spectral instabilities, a low numerical aperture lens was used for seed laser collimation at a working distance of ~1 cm. A low lens collection efficiency resulted in 12 mW seed power incident on the tapered amplifier, which near its 860 nm gain peak emitted 1.25 W at a current of 2.0 A. Typical pump power measured at the input facet of a 6 mm long periodically poled $LiNbO_3$ (PPLN) crystal was 820 mW. The field-poled, z-cut crystal had a domain period of 22.6 μm and was oriented ~10° relative to the beam to achieve wideband quasi-phase-matching in the 4.3-4.6 μm range. With 220 mW of incident power at 1064 nm, a maximum of 8.0 μW was measured at 4.5 μm. The amplifier was typically operated to produce DFG power of ~3.0 μW, adequate for all of the spectroscopic measurements described below.

The spectrum of the seeded amplifier was monitored with an optical spectrum analyzer and a Fabry-Perot interferometer. The linewidth was less than the 50 MHz resolution of the interferometer. Coarse and fine wavelength adjustments were carried out via seed laser temperature and bias current settings, respectively. Frequency scans were made by superimposing a 30 mA peak-to-peak triangular waveform at ~10 Hz on the seed laser bias current, resulting in a continuous mode-hop-free frequency sweep range of 80 GHz. An additional f=2 kHz sinusoidal waveform was used for frequency modulation during scans, with up to 11 GHz peak-to-peak frequency modulation amplitude. Frequency sweep and modulation were accompanied by linear modulation of the seed power. This modulation was greatly suppressed by the clamped input-versus-output power transfer function of the tapered amplifier operated in a regime close to saturation. Because of the relatively low seed power, however, the saturation was incomplete and the nonlinearity of the amplifier power transfer function produced second harmonic of the modulation frequency, causing a weak rolling baseline in the 2f infrared spectra. This effect can be reduced by increasing the seed power. Another undesirable effect observed initially was weak etalon interference between the two facets of the tapered amplifier. This interference resulted in the DFG power modulation during scan, which masked

the gas absorption signal. During 80 GHz scan, the seed wavelength tuned across four amplifier etalon fringes, spaced by approximately 20 GHz. To eliminate this effect, we synchronously modulated the amplifier current with the ramp used for seed laser frequency scans. This caused, via temperature and carrier density induced index variation, a proportional scan of etalon fringe wavelength. With proper adjustment of the ramp amplitude (~200 mA) and phase, the etalon fringe wavelength excursion matched that of the seed laser, and the power modulation caused by interference was eliminated. Improved antireflection coating of the diode amplifier chip could reduce etalon effects making the injection current modulation unnecessary.

The intensity noise spectra of both DFG sources were measured using a fast Fourier transform spectrum analyzer, and the results are shown in Figure 2. Initially, the noise in the 3.2 μm source below 3 kHz was determined by the cavity locking noise. In later experiments, a servo loop was used to reduce it. A portion of the IR beam was focused onto a room-temperature InAs reference detector, and the feedback adjustment of the diode laser power was performed by an acousto-optic modulator. This allowed the effects of the Nd:YAG buildup cavity noise, the amplitude modulation of the diode laser resulting from frequency tuning, and background fringes to be cancelled out. No attempt was made to suppress noise in the 4.6 μm source which was caused primarily by technical noise in the tapered amplifier current supply.

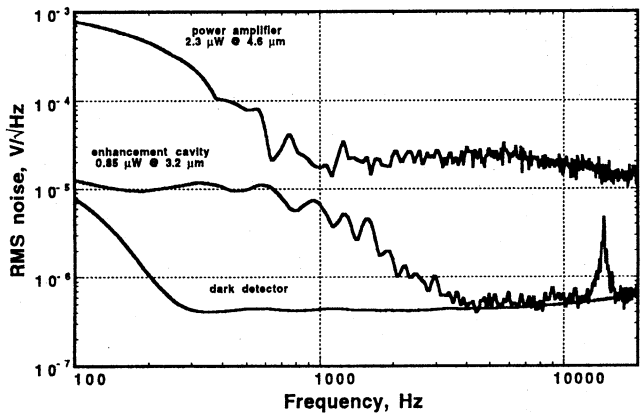

Figure 2. Power spectral density of the IR intensity noise measured with a fast Fourier transform analyzer. Liquid-nitrogen-cooled InSb detector was used. The noise plateau below 3 kHz in the 3.2 μm DFG source is due to the buildup cavity locking noise. The 4.6 μm source was dominated by technical noise in the current supply of the tapered amplifier.

The sources were used to detect methane, carbon monoxide, nitrous oxide, and carbon dioxide in natural air. Figure 3, left, shows direct absorption spectrum of the methane in natural air at 80 torr in a 1 m single-pass cell. It was acquired using a signal-averaging bandwidth of 1 Hz, and IR power stabilization (A). Atmospheric pressure-broadened methane in the laboratory air between the power stabilizer beamsplitter and the sample cell is visible in the baseline trace (B). The baseline slope is due to interference from a secondary reflection from the power stabilizer beamsplitter. The bottom trace is the difference between A and B and only shows the signal from the cell. Based upon the observed signal-to-noise ratio, a detection limit (signal-to-noise ratio of 1) of 12 ppb·m/√Hz can be determined; it is in good agreement with the measured InAs detector noise.

The ambient CO and N_2O were monitored over 4.2 m open path between the mixing crystal and signal detector. Figure 3, right, shows wavelength-modulation 2f spectra of the R(6) fundamental of CO near 2169 cm^{-1} in air, and in a reference sample. The sample had ~3 torr of CO mixed with air at atmospheric pressure in a 10 cm cell, resulting in 93% peak absorption. The 2f absorption signal was monitored to allow easy visual comparison of position and width of the signal and reference absorption peaks. The vertical line at the center indicates reversal of the

frequency sweep which was approximately 20 GHz. Both traces are 100 sweep averages, resulting in the noise bandwidth of 2.5 Hz. The rolling baseline in the air trace is a result of synchronous amplitude modulation in the tapered amplifier as mentioned above. It is asymmetric because of weak thermal modulation in the amplifier caused by the frequency sweep and delayed in time. Magnitudes of absorption peaks in the top trace suggest that the CO concentration in laboratory air is ~360 ppb. The root-mean-square noise in the top trace corresponds to equivalent column density of 5 ppb·m/√Hz for CO in air at atmospheric pressure.

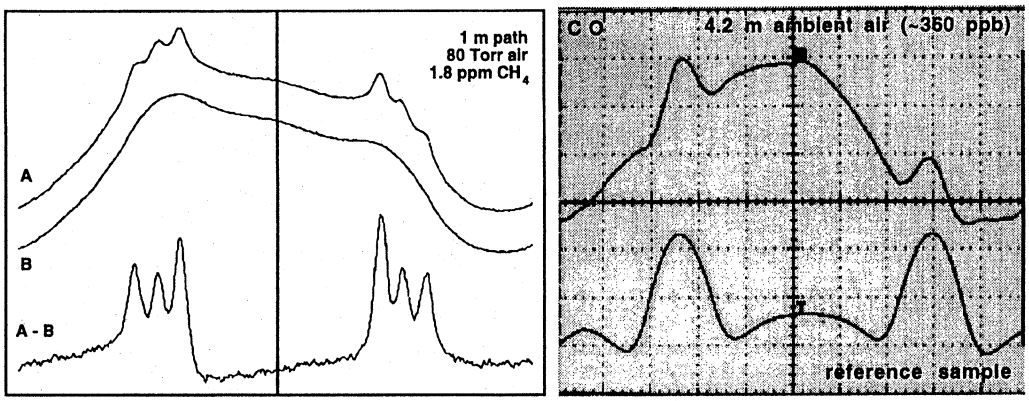

Figure 3. Direct-absorption spectrum of methane near 3086 cm^{-1} (**left**) and wavelength-modulation 2*f* spectrum of carbon monoxide near 2169 cm^{-1} (**right**) in natural air acquired using 1 μW probe power. Equivalent noise bandwidth was 1 Hz and 2.5 Hz, respectively. The frequency sweep is reversed at the center of each plot. Detection limits of 12 and 5 ppb·m/√Hz can be inferred.

In summary, we have performed sensitive detection of the methane, carbon monoxide, and nitrous oxide in natural air using all-diode-pumped CW tunable difference-frequency generation at 3.2 μm and 4.6 μm at room temperature. With no cryogenic components, the detection limits in air of 12 ppb·m/√Hz for methane and 5 ppb·m/√Hz for carbon monoxide were determined based on the measured signal-to-noise ratio. The maximum tuning range of 200 cm^{-1} with less than 50 MHz linewidth, and output power of at least 6 μW was observed at both wavelengths. The tuning range can be extended for the detection of NO and SO_2. From the standpoint of spectroscopic trace gas detection, the diode-pumped mid-infrared DFG proves to be a useful alternative lead-salt diode lasers [1], and near-infrared overtone detection [2], especially when the overtone bands are either weak, or not accessible directly by near-IR laser diodes, or overlap with strong absorption bands of water vapor.

The work was supported in part by the National Science Foundation, National Aeronautics and Space Administration, Office of Naval Research, U. S. Department of Commerce, and Robert A. Welch Foundation.

1. C. R. Webster, R. D. May, C. A. Trimble, R. G. Chave, and J. Kendall, *Appl. Opt.* 33 (**3**) 454-472 (1994)
2. K. Uehara and H. Tai, *Appl. Opt.* 31 (**6**) 809-814 (1992)
3. D. Z. Garbuzov, R. U. Martinelli, R. J. Menna, P. K. Yourk, H. Lee, S. Y. Narayan, and J. C. Connolly, *Appl. Phys. Lett.* 67 (**10**) 1346-1348 (1995)
4. A. J. Henderson, M. J. Padgett, J. Zhang, W. Sibbett, and M. H. Dunn, *Opt. Lett.* 20 (**9**) 1029-1031 (1995)
5. A. S. Pine, *J. Opt. Soc. Am.* 66 (**2**) 97-108 (1976)
6. U. Simon, S. Waltman, I. Loa, L. Hollberg, and F. Tittel, *J. Opt. Soc. Am. B* 12 (**2**) 323-327 (1995)
7. K. P. Petrov, S. Waltman, U. Simon, R. F. Curl, F. K. Tittel, E. J. Dlugokencky, and L. Hollberg, *Appl. Phys. B* 61 (1995)
8. K. P. Petrov, L. Goldberg, W. K. Burns, R. F. Curl, and F. K. Tittel, *submitted to Opt. Lett.* (1995)